



**HAL**  
open science

## Microfluidic synthesis and assembly of reactive polymer beads to form new structured polymer materials

Nicolas Berton, Michel Bouquey, Christophe Serra, Laurent E. Prat, Georges Hadziioannou

► **To cite this version:**

Nicolas Berton, Michel Bouquey, Christophe Serra, Laurent E. Prat, Georges Hadziioannou. Microfluidic synthesis and assembly of reactive polymer beads to form new structured polymer materials. Chemical Engineering Journal, 2008, 135 (suppl. 1), pp.S93-S98. 10.1016/j.cej.2007.07.043 . hal-00467130

**HAL Id: hal-00467130**

**<https://hal.science/hal-00467130>**

Submitted on 23 Apr 2024

**HAL** is a multi-disciplinary open access archive for the deposit and dissemination of scientific research documents, whether they are published or not. The documents may come from teaching and research institutions in France or abroad, or from public or private research centers.

L'archive ouverte pluridisciplinaire **HAL**, est destinée au dépôt et à la diffusion de documents scientifiques de niveau recherche, publiés ou non, émanant des établissements d'enseignement et de recherche français ou étrangers, des laboratoires publics ou privés.

# Microfluidic synthesis and assembly of reactive polymer beads to form new structured polymer materials

Michel Bouquey<sup>a</sup>, Christophe Serra<sup>a,\*</sup>, Nicolas Berton<sup>a</sup>,  
Laurent Prat<sup>b</sup>, Georges Hadziioannou<sup>a</sup>

<sup>a</sup> Laboratoire d'Ingénierie des Polymères pour les Hautes Technologies, CNRS UMR 7165, ECPM, 25 rue Becquerel, 67087 Strasbourg Cedex 2, France

<sup>b</sup> Laboratoire de Génie Chimique, CNRS UMR 5503, INPT, 5 rue Paulin Talabot, 31106 Toulouse Cedex 1, France

---

## Abstract

Monodisperse and size-controlled polymer particles were produced without surfactant or washcoat from O/W monomer emulsions and “on the fly” polymerization under UV irradiation in a very simple needle/tubing system. The effect of the viscosity of the continuous phase on the size of final particles was investigated. The capillary number ratio was found to be relevant to predict the size of the droplets. A relation between dimensionless numbers predicts particle diameter as a function of the needle inner diameter and both velocity and viscosity ratios of continuous and dispersed phases. A functional comonomer was incorporated in the monomer phase so as to obtain polymer microparticles bearing reactive groups on their surface. Polymer beads necklaces were thus formed by linking polymer particles together.

*Keywords:* Microfluidic; Monodisperse polymer particles; Particles assembly; Photopolymerization; Microreactor

---

## 1. Introduction

So far, polymer particles were mainly prepared by either heterogeneous polymerization processes (emulsion, suspension, supercritical fluid) or by precipitation processes in a non-solvent. These two processes lead to polymer particles having a different size domain, but they induce a large particle size distribution. Recently, microfluidic processes have been considered because of their unique capacity to generate thousands of microdroplets with a very narrow size distribution. Indeed, if the microdroplets generated are polymerizable media, it is possible to obtain thousands of polymer particles with well-defined characteristics like size, shape and morphology. Polymer beads [1–3], disks and plugs [3,4] were thus synthesized. Microfluidics also enable to form multiphase droplets [5] from which partial polymer spheres [6], Janus [7] and ternary polymer particles [8] were obtained.

The first microfluidic emulsification systems were derived from the membrane emulsification process [9]. By forcing a to-be-dispersed phase into a continuous phase through microchannels, microchannel emulsification [10,11] and straight-through

microchannel emulsification systems [12] were able to produce monodisperse microdroplets with diameters in the range of 1–100  $\mu\text{m}$ . The production rates of droplets were however low. A method was proposed to form monodisperse droplets at a capillary tip in a co-flowing immiscible fluid [13]. Recently, emulsification techniques using a micro-T-junction [4,5,7,14–17] and microfluidic flow-focusing devices (MFFD) with rectangular channels have been developed for the production of monodisperse droplets [3,18–20] or bubbles [21,22] with diameters typically varying from 10 to several hundred micrometers. The affinity of the droplet phase for the material of the system can cause “inverted droplets” when the droplets wet the walls or even “phase inversion” when the liquid to be dispersed becomes a continuous phase [7]. Since the walls are usually hydrophobic (glass or PDMS), inverted droplets are likely to be observed in oil-in-water emulsions and a washcoat is necessary to make the surface hydrophilic so as to avoid that droplets wet the walls. An axisymmetric microfluidic flow-focusing device (AFFD) has been realized to avoid contact with walls by delivering droplets in the middle of the channel [23]. However, the fabrication of these systems is complicated and they can be clogged with polymer debris. These drawbacks can be overcome through the use of a needle to generate droplets inside a tubing. Such a system has been reported recently [24,25] and was

---

\* Corresponding author.

E-mail address: SerraC@ecpm.u-strasbg.fr (C. Serra).

found to exhibit similar behavior to that of standard microfluidic devices [24].

Diameters of droplets formed in microfluidic devices depend mainly upon the dimension of the system and the flow rates of the continuous and dispersed phases [7,15,17,24]. However there is little information regarding the role of the viscosity in droplets formation. Seo et al. [3] tested monomer solutions with different viscosities, but the viscosity of the dispersed phase was imposed by the nature of the monomer. Controlling the size of the droplets by varying the viscosity of the continuous phase would be much more convenient. Since droplets formation is due to interfacial tension forces [11,14,20], surfactants are usually added in order to stabilize droplets. But an emulsification system working without surfactant would be more versatile regarding the kind of monomer. Furthermore, the absence of surfactant would favor interfacial reactions, which is of particular interest for particles assembly.

The work presented here aims at the synthesis of polymer beads necklaces. A three-step procedure is described. First, O/W functional monomer droplets are formed without surfactant or washcoat. They are then polymerized “on the fly” under UV irradiation. Polymer beads are finally stacked and linked together. It was found that increasing the viscosity of the carrier fluid is a solution to the problem of inversed droplets generation. The effect of the viscosity of the continuous phase on droplets diameter is investigated.

## 2. Experimental

### 2.1. Droplets formation

Dispersed phase: monomer: methyl methacrylate (MMA) 87 wt.%; cross-linker: dimethacrylate ethylene glycol (DIMAEG), 5 wt.%; functional comonomer: glycidyl methacrylate, 3 wt.%; photoinitiator: Irgacure 907, 5 wt.%. The photoinitiator was provided by Ciba, DIMAEG and glycidyl methacrylate were purchased from Aldrich. MMA was purchased from Acros Organics and used without destabilization. The viscosity of the dispersed phase as measured with a Ubbelohde capillary viscosimeter (type 531 10 I, Schott Geräte) was equal to 0.72 cP.

Continuous phase: aqueous solution of methyl cellulose in distilled water. The viscosity was measured with a rheometer Rheo RV8 (spindle 6, 50 rpm), and varied with the amount of methyl cellulose from 350 to 1450 cP.

Two syringe pumps (Harvard PHD 2000) were used to regulate the flow rates of the two phases. The dispersed phase was injected into the continuous one thanks to a system that is made of a T-junction, an outlet PTFE tubing (1/16 in. i.d.), and a needle positioned directly in the axis of the tubing (Fig. 1). We used 25-gauge and 32-gauge needles, with inner diameters of 260 and 110  $\mu\text{m}$ , respectively.

### 2.2. Photopolymerization

The PTFE tubing was wrapped in an aluminum foil into which lightguides were introduced. Thus, the monomer droplets were

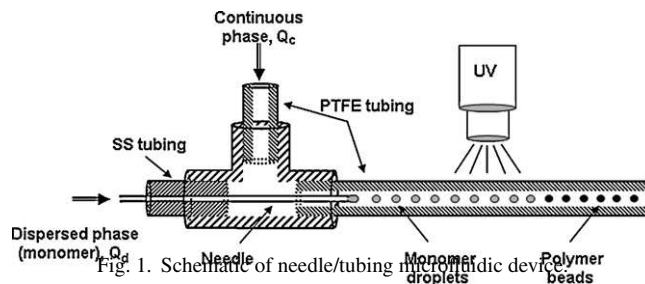


Fig. 1. Schematic of needle/tubing microfluidic device.

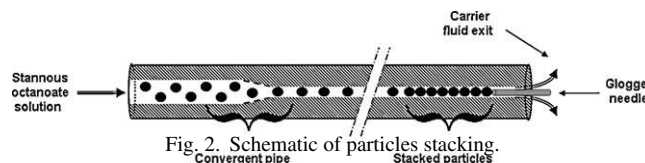


Fig. 2. Schematic of particles stacking.

polymerized “on-the-fly” by free radical polymerization in the PTFE tubing under UV irradiation. The UV source (Hamamatsu Lightningcure LC8) operated at  $\lambda = 365 \text{ nm}$ , which corresponds to the maximum of absorbance of the photoinitiator added to the monomer phase.

### 2.3. Linkage

Once polymerized, particles were washed with an aqueous solution of stannous octanoate and stacked with a glogged needle in such a way that each microparticle got into contact with two other microparticles (Fig. 2). The tubing containing the particles was then heated for 1 h at 80  $^{\circ}\text{C}$  to promote the linkage reaction.

### 2.4. Measurement of diameter

The diameters of particles were measured using an optical microscope. The polymerized particles were collected at the outlet of the channel without being assembled. Average diameters were calculated over samples of at least 50 polymer particles. Polymer particles have diameters 8% smaller than those of monomer droplets, due to the higher density of polymers.

## 3. Viscosity effect and capillary numbers

Two dimensionless numbers are generally used to describe the hydrodynamic conditions, the Reynolds number  $Re = \rho VD/\mu$ , and the capillary number  $Ca = \mu V/\gamma$ , where  $\rho$  is the density of the liquid,  $V$  the average velocity,  $D$  the characteristic length scale of the system (here the diameter of the tubing),  $\mu$  the viscosity of the fluid and  $\gamma$  is the interfacial tension. All experiments were run at low Reynolds numbers ( $10^{-3} \leq Re \leq 10^{-2}$ ), which is usual in microfluidic devices but had not been tested for the present needle/tubing system since Quevedo et al. [24] worked at relatively higher Reynolds ( $1 \leq Re \leq 170$ ). Two capillary numbers  $Ca_c$  and  $Ca_d$  can be defined for the continuous and dispersed phases. The capillary number represents the

ratio of viscous forces to interfacial tension forces and usually applies to the dispersed phase. Here, an outer capillary number is also useful to take into account the effect of the continuous phase. We define  $Ca_c = (\mu_c 4 Q_c) / (\gamma \pi D_{\text{tube}}^2)$  and  $Ca_d = (\mu_d 4 Q_d) / (\gamma \pi D_{\text{cap}}^2)$ , where  $\mu_c$  and  $\mu_d$ ,  $Q_c$  and  $Q_d$  are respectively the viscosities and flow rates of the continuous and dispersed phase,  $D_{\text{tube}}$  the tube inner diameter and  $D_{\text{cap}}$  is the capillary inner diameter. We worked at low  $Ca_c$ , very low  $Ca_d$  ( $0.01 \leq Ca_c \leq 0.1$ ;  $5 \times 10^{-6} \leq Ca_d \leq 5 \times 10^{-4}$ ) and high viscosity ratio  $\mu_c/\mu_d$ . In such conditions, we operated in the dripping mode [25]. The jetting mode, sometimes observed in microfluidic devices [3,6,25] was unlikely to occur. Droplets were formed at the exit of the capillary, and therefore no satellite droplets were expected [26].

Several authors have already studied the effect of the flow rates of both continuous and dispersed phases on the diameter of droplets formed in microfluidic devices [3,7,15,17,24]. It is well known that for given continuous and dispersed solutions, the particles diameter decreases when the flow rate of the continuous phase increases and when the flow rate of the dispersed phase decreases. Here, we observed similar behavior. We also found that only the ratio of the flow rates  $Q_c/Q_d$  between continuous and dispersed phase determines particles diameter.

We studied the variation of the particles diameter for different viscosities of the continuous phase. At high ratio  $Q_c/Q_d$  and at a given viscosity  $\mu_c$ , the diameter of the particles tends to a minimum value. The minimum value decreases with increasing viscosity (Fig. 3), due to the higher shear applied to the dispersed phase. However, if the viscosity is higher than 800 cP, the minimum diameter stabilizes around 260  $\mu\text{m}$ , which corresponds to the dimension of the needle internal diameter. This is consistent with the results obtained by Cygan et al. [17] and Quevedo et al. [24], where the geometry limited the threshold value as well. However smaller particles were produced by using a thinner needle (Fig. 4).

It should be noticed that reported experiments had only studied the case of high dispersed phase viscosity and had found that viscosity did not influence droplets diameter [25]. The explanation for this phenomenon was that the formation of droplets with high viscosity is close to drop formation in quiescent fluid. We

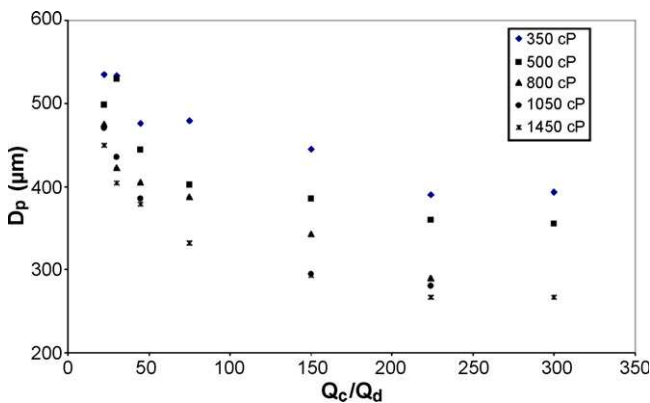


Fig. 3. Variation of the average diameter of polymer particles produced with a gauge-25 needle for different viscosities of the continuous phase: 350, 500, 800cP, 1050 and 1450 cP.

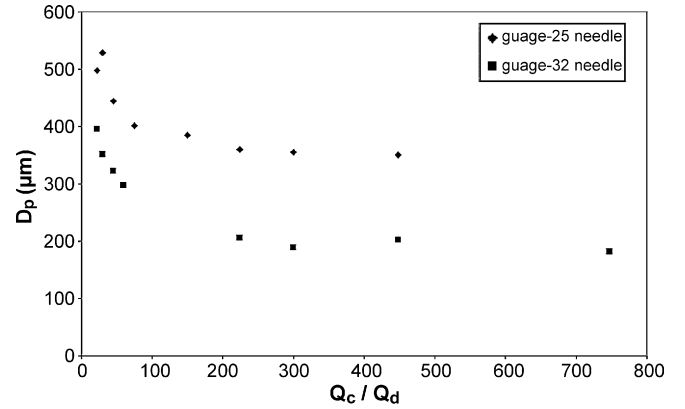


Fig. 4. Average diameter of polymer particles produced with two different needles (viscosity of the continuous phase is equal to 500 cP).

demonstrate here that it is no longer true at high viscosity ratio  $\mu_c/\mu_d$ , even at low velocity of the continuous phase. It seems clear that viscous forces must be taken into account in the formation of droplets as the shear stress imposed by the surrounding flowing continuous phase is counterbalanced by the interfacial forces. It is therefore interesting to use the capillary number that is the ratio between viscous forces and interfacial tension. In a numerical study of drop formation at a vertical capillary tube, Zhang and Stone [26] have shown that the capillary number of the continuous phase plays an important role in the drop formation. An increase in this parameter leads to smaller drops, longer breaking length and shorter breaking time. Here, analogously with the flow rates ratio  $Q_c/Q_d$ , the ratio of the capillary numbers  $Ca_c/Ca_d$  is defined according to Eq. (1) below:

$$\frac{Ca_c}{Ca_d} = \frac{\mu_c V_c}{\mu_d V_d}, \quad (1)$$

where  $\mu_c$  and  $\mu_d$  are respectively the viscosity of the continuous and dispersed phase, and  $V_c$  and  $V_d$  are respectively the average velocity of each phase. Data of Fig. 3 plotted with respect to  $Ca_c/Ca_d$  lead to a master curve (Fig. 5). Thus the ratio of the capillary numbers of the continuous and dispersed phases  $Ca_c/Ca_d$  is relevant to control the particles diameter.

However, using two needles, we get two different master curves because the thinner the needle, the smaller are particles (Fig. 6). Since the needle inner diameter is a key parameter, it is convenient to define a dimensionless particle diameter  $D_p/D_{\text{cap}}$ , where  $D_p$  is the average particle diameter and  $D_{\text{cap}}$  is the inner diameter of the capillary. By plotting all the previous data as the variation of  $D_p/D_{\text{cap}}$  versus  $Ca_c/Ca_d$  one obtains a unique dimensionless master curve (Fig. 7), which leads to an empirical relation describing the particles size in such a microfluidic device:

$$\text{Ln} \left( \frac{D_p}{D_{\text{cap}}} \right) = -0.22 \text{Ln} \left( \frac{Ca_c}{Ca_d} \right) + 2.07. \quad (2)$$

As it can be seen in Fig. 5, given the capillary diameter and the viscosity, two regimes of droplets formation are identified: a decreasing zone where particles diameter decreases with increasing the capillary numbers ratio, and a threshold zone at high values of the capillary numbers ratio. Eq. (2) is only

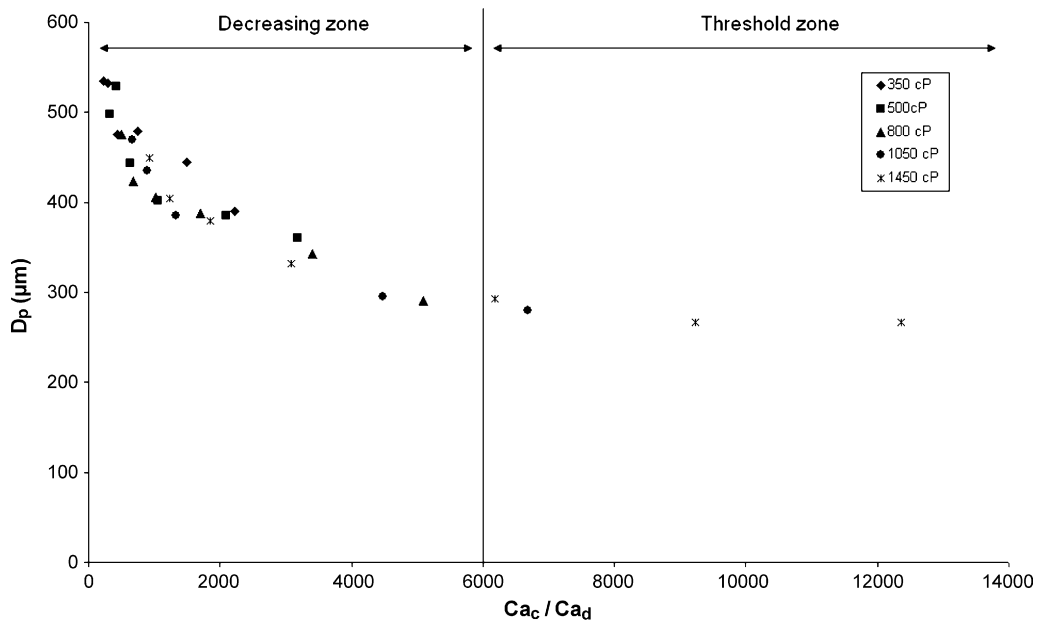


Fig. 5. Variation of the average diameter  $D_p$  of polymer particles produced with a gauge-25 needle for different viscosities of the continuous phase. Experimental data are the same as in Fig. 3.

valid in the decreasing zone. It must be noticed that it corresponds to the adequate zone for the production of monodisperse droplets. Indeed, in the first regime, the coefficient of variation  $CV = \sigma/D_p$ , where  $\sigma$  is the standard deviation and  $D_p$  the average particle diameter, remains in the range of 2–5%. On the contrary, in the threshold zone ( $D_p/D_{cap}$  close to 1) emulsions tend to become polydisperse, i.e.  $CV > 5\%$  (Fig. 8).

A relation similar to Eq. (2) was found in the case of fragmentation of droplets under shear stress [27]. The effect of viscosity ratio was studied at constant shear rate. Monodisperse droplets were obtained, with diameters varying as a function of the viscosity ratio of continuous to dispersed phases. The exponent was equal to  $-0.2$  as well, although the mechanism seems to be different. There was no velocity ratio entering the description of the system since droplets were already pre-formed. Besides, Rayleigh instability was involved in the mechanism of droplets fragmentation. In our experiments, droplets are formed close to the needle exit, so we do not observe any fragmentation of

a thread. However the mechanism of droplets formation could be similar since in both cases a shear stress is exerted by the continuous phase.

Droplet formation is also driven by interfacial tension. However we may expect the exponent in Eq. (2) not to be affected by this parameter. For different values of interfacial tension, we should get parallel lines in Fig. 7 as experimentally observed by Cramer et al. [25] when varying the continuous phase velocity for two different values of interfacial tension at a constant dispersed phase velocity. As predicted by several models [26,28] the droplet diameter varies linearly with respect to the interfacial tension. Thus the offset value in Eq. (2) is expected to be proportional to the interfacial tension. This was indirectly observed when looking at the influence of the weight content of GMA introduced in the dispersed phase (Fig. 9). Globally the higher the concentration of GMA, the lower is the offset value. GMA bears an epoxy group which affinity towards water should place it at the surface of the droplet reducing its interfacial tension.

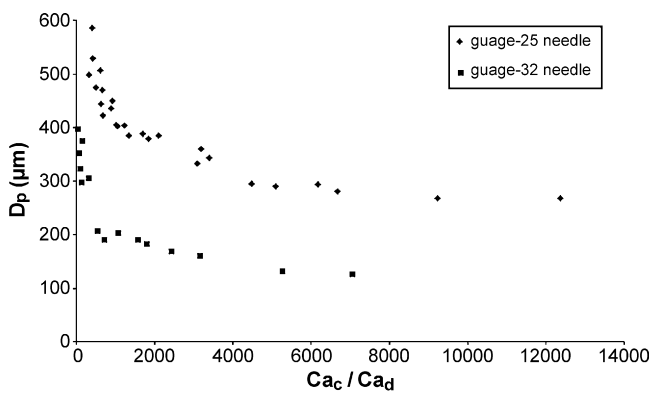


Fig. 6. Master curves of the average particle diameter  $D_p$  obtained using two different needles.

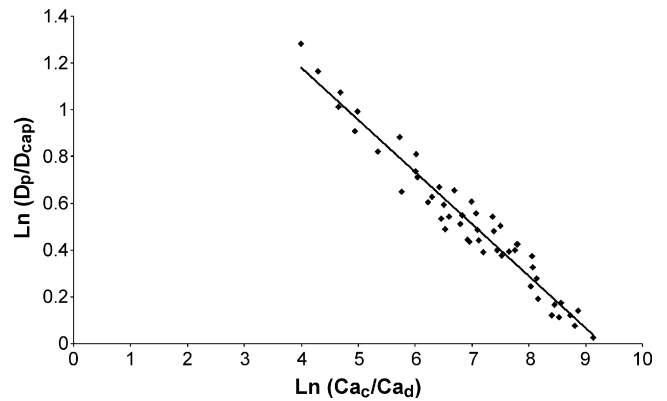


Fig. 7. Master curve of the dimensionless particle diameter obtained with capillaries of different sizes and with different viscosities of the continuous phase.

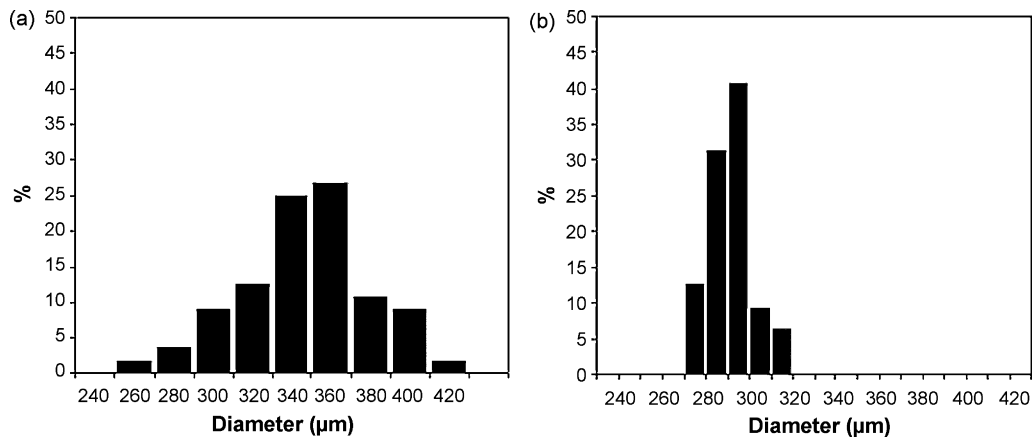


Fig. 8. Typical size distribution of particles diameters obtained in (a) the threshold zone and (b) the decreasing zone. CVs are equal to 9% (a) and 3% (b).

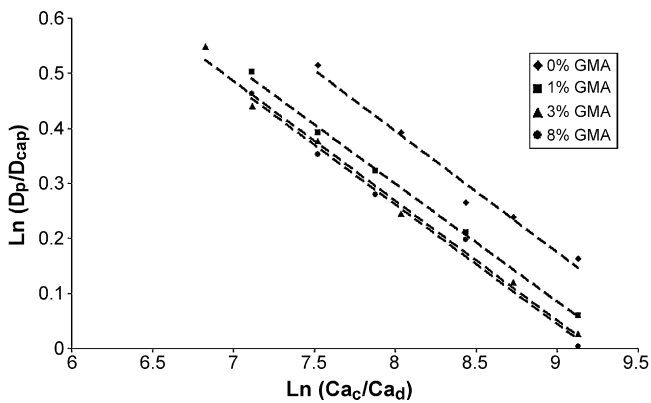


Fig. 9. Influence of the weight content of GMA on the variation of the dimensionless particle diameter.

However it is noteworthy that the offset value does not change for weight content of GMA greater than 3% which might correspond to the minimum value of the surface tension obtained when the whole droplet surface is covered with epoxy groups.

#### 4. Synthesis of polymer beads necklaces

Glycidyl methacrylate was copolymerized with DIMAEG and MMA during the free radical polymerization step initiated by UV exposure, leading to statistical copolymers. MMA monomers were in large excess in the initial dispersed phase, so polymer chains contain 2 glycidyl methacrylate units and 3 DIMAEG units for 100 MMA units. The presence of a cross-linker (DIMAEG) aimed at the formation of insoluble and infusible particles while the presence of glycidyl methacrylate monomers led to polymer beads bearing glycidyl groups on their surface. Reactive polymer particles were thus obtained and were stacked in a tubing (Fig. 2). Particles must have diameters close to the tubing inner diameter, otherwise they arrange in quincunx. To avoid such arrangement we used a convergent pipe (Fig. 2). They must also be completely polymerized to avoid deformation under pressure during the stacking. The chemical reaction between glycidyl groups on the surface of particles put together into contact was promoted in aqueous media using stan-

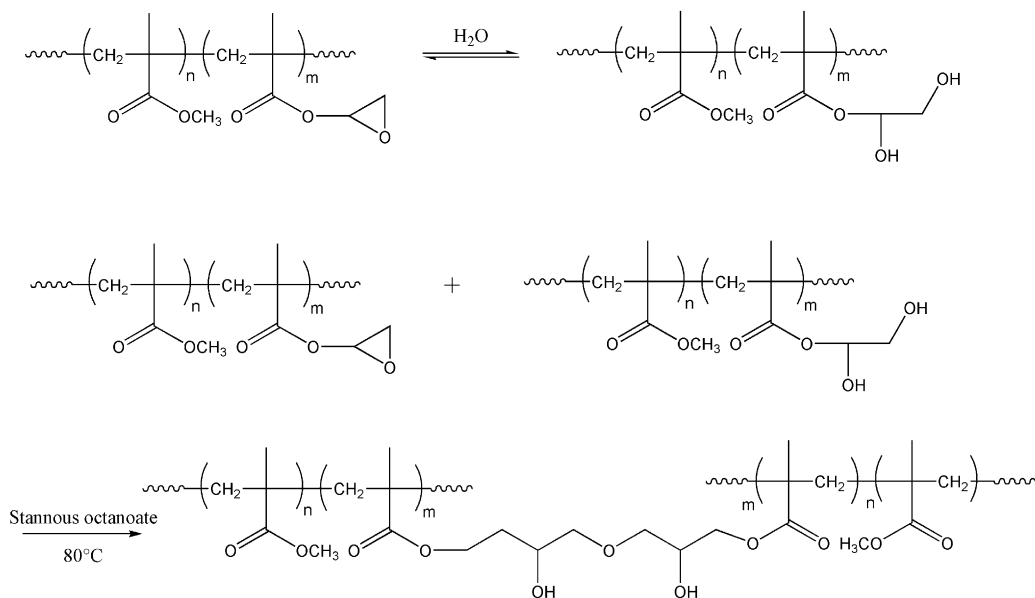


Fig. 10. Principle of chemical reaction between poly(methyl methacrylate-co-glycidyl methacrylate) on particles surface.

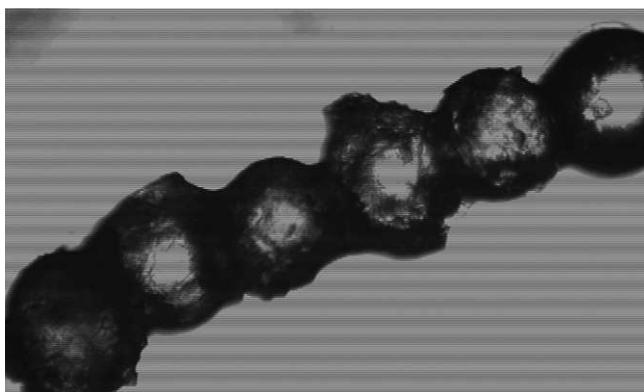


Fig. 11. Polymer beads necklace.

nous octanoate as a catalyst [29] (Fig. 10). Covalent bonds were formed between particles. It resulted in the formation of polymer beads necklaces (Fig. 11). Necklaces are however quite fragile and break under low shear. Such necklaces are totally new polymer structures.

## 5. Conclusion

In this work, it was demonstrated that the use of a simplified microfluidic device allows the synthesis of new structured polymer materials. O/W monomer emulsions are produced without surfactant or washcoat in a needle/tubing device. The viscosity of the continuous phase is useful to control droplets size and therefore polymer particles size. It appears that the ratio of the capillary numbers of the continuous and dispersed phases is a key parameter. The diameter of the needle seems to be a limiting factor and it is expected that the use of thinner capillaries will lead to smaller droplets. An empirical relation enables to predict particle size. In situ photopolymerization of monomer droplets leads to monodisperse polymer particles that are then stacked and linked together via a reaction between the reactive groups of the functional comonomers, resulting in covalent bonds between particles and therefore in the formation of a polymer beads necklace. The linkage still has to be strengthened. The use of low T<sub>g</sub> monomers would lead to less rigid particles and therefore increase the contact area between particles during the stacking step, which should result in stronger linkage. By varying the nature of the monomer or the amount of cross-linking agent, and by forming alternate necklaces through the alternate formation of different polymerizable microdroplets, it will be possible to adjust some of the physical properties of each bead. We believe that the use of microfluidic devices is a promising way of synthesizing polymer beads necklaces with a large range of morphologies and properties which may found applications as fillers or as patterned templates.

## Acknowledgement

Authors acknowledge the French Ministry of Higher Education and Research for having funded this work through the grant ANR no. NT05-1\_45715.

## References

- [1] S. Sugiura, M. Nakajima, H. Itou, M. Seki, *Macromol. Rapid Commun.* 22 (2001) 773–778.
- [2] F. Ikkai, S. Iwamoto, E. Adachi, M. Nakajima, *Colloid Polym. Sci.* 283 (2005) 1149–1153.
- [3] M. Seo, Z. Nie, S. Xu, M. Mok, P.C. Lewis, R. Graham, E. Kumacheva, *Langmuir* 21 (2005) 11614–11622.
- [4] D. Dendukuri, K. Tsoi, T.A. Hatton, P.S. Doyle, *Langmuir* 21 (2005) 2113–2116.
- [5] J.D. Tice, H. Song, A.D. Lyon, R.F. Ismagilov, *Langmuir* 19 (2003) 9127–9133.
- [6] Z. Nie, S. Xu, M. Seo, P.C. Lewis, E. Kumacheva, *J. Am. Chem. Soc.* 127 (2005) 8058–8063.
- [7] T. Nisisako, T. Torii, T. Higuchi, *Chem. Eng. J.* 101 (2004) 23–29.
- [8] Z. Nie, W. Li, M. Seo, S. Xu, E. Kumacheva, *J. Am. Chem. Soc.* (2006) published on web.
- [9] T. Nakashima, M. Shimizu, M. Kukizaki, *Key Eng. Mater.* 61/62 (1991) 513–516.
- [10] T. Kawakatsu, Y. Kikuchi, M. Nakajima, *J. Am. Oil Chem. Soc.* 74 (1997) 317–321.
- [11] S. Sugiura, M. Nakajima, S. Iwamoto, M. Seki, *Langmuir* 17 (2001) 5562–5566.
- [12] I. Kobayashi, M. Nakajima, K. Chun, Y. Kikuchi, H. Fujita, *AIChE J.* 48 (2002) 47–56.
- [13] P.B. Umbanhowar, V. Prasad, D.A. Weitz, *Langmuir* 16 (2000) 347–351.
- [14] T. Thorsen, R.W. Roberts, F.H. Arnold, S.R. Quake, *Phys. Rev. Lett.* 86 (2001) 4163–4166.
- [15] T. Nisisako, T. Torii, T. Higuchi, *Lab Chip* 2 (2002) 24–26.
- [16] S. Okushima, T. Nisisako, T. Torii, T. Higuchi, *Langmuir* 20 (2004) 9905–9908.
- [17] Z.T. Cygan, J.T. Cabral, K.L. Beers, E.J. Amis, *Langmuir* 21 (2005) 3629–3634.
- [18] S.L. Anna, N. Bontoux, H.A. Stone, *Appl. Phys. Lett.* 82 (2003) 364–366.
- [19] Q. Xu, M. Nakajima, *Appl. Phys. Lett.* 85 (2004) 3726–3728.
- [20] Y.C. Tan, V. Cristini, A.P. Lee, *Sensor. Actuat. B: Chem.* 114 (2006) 350–356.
- [21] A.M. Ganan-Calvo, J.M. Gordillo, *Phys. Rev. Lett.* 87 (2001) 274501.
- [22] P. Garstecki, M.J. Fuerstman, G.M. Whitesides, *Phys. Rev. Lett.* 94 (2001) 234502.
- [23] S. Takeuchi, P. Garstecki, D.B. Weibel, G.M. Whitesides, *Adv. Mater.* 17 (2005) 1067–1072.
- [24] E. Quevedo, J. Steinbacher, D.T. McQuade, *J. Am. Chem. Soc.* 127 (2005) 10498–10499.
- [25] C. Cramer, P. Fischer, E.J. Windhab, *Chem. Eng. Sci.* 59 (2004) 3045–3058.
- [26] D.F. Zhang, H.A. Stone, *Phys. Fluids* 9 (1997) 2234–2242.
- [27] C. Mabille, F. Leal-Calderon, J. Bibette, V. Schmitt, *Europhys. Lett.* 61 (2003) 708–714.
- [28] H. Oguz, A. Prosperetti, *J. Fluid Mech.* 257 (1993) 111–145.
- [29] C.A. May, *Epoxy Resins, Chemistry and Technology*, 2nd ed., M. Dekker, New York, 1988.